Part Removal of 3D Printed Parts

by

Mateo Peña Doll

SUBMITTED TO THE DEPARTMENT OF MECHANICAL ENGINEERING IN PARTIAL FULFILLMENT OF
THE REQUIREMENTS FOR THE DEGREE OF

BACHELOR OF SCIENCE IN MECHANICAL ENGINEERING
AT THE
MASSACHUSETTS INSTITUTE OF TECHNOLOGY

JUNE 2014
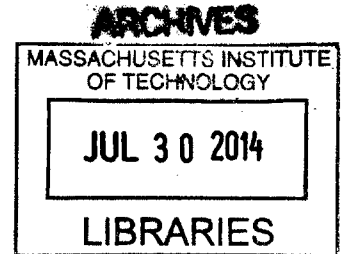
Signature redacted

Signature of Author:_____

Department of Mechanical Engineering
May 9, 2014

Signature redacted

Certified by: _____

Sanjay E. Sarma
Professor of Mechanical Engineering
Thesis Supervisor

Signature redacted

Accepted by: _____

Annette Hosoi
Associate Professor of Mechanical Engineering
Undergraduate

1

This page is intentionally left blank

Part Removal of 3D Printed Parts

by

Mateo Peña Doll

Submitted to the Department of Mechanical Engineering on May 9, 2014 in Partial Fulfillment of the Requirements for the Degree of Bachelor of Science in Mechanical Engineering

ABSTRACT

An experimental study was performed to understand the correlation between printing parameters in the FDM 3D printing process, and the force required to remove a part from the build platform of a 3D printing using a patent pending, New Valence Robotics Corporation technology for automated part removal of 3D printed parts. These correlations are used to optimize printing parameters to minimize the force required for removal, without decreasing the quality of the printed object. The bed (build platform) temperature, extruder temperature, bed temperature during the removal process (removal bed temperature), and first layer height of prints on a Solidoodle 2 3D printer were varied independently. For each parameter tested, the orientation of the part being removed, an ellipse, was oriented with its major axis parallel and perpendicular to the blade edge. On average, the parallel orientation incurred larger loads on the removal blade mechanism by about 10 to 20%. The first layer height parameter had the largest effect on the required force, with a linear trend from 47.62 ± 8.98 N at a layer height of 0.47 ± 0.02mm, to 123.92 ± 22.93 N at a layer height of 0.18 ± 0.01mm (parallel orientation). The extruder temperature parameter had a large effect on the removal force when raised close to the glass transition temperature of the build platform material, a PEI fill. At an extruder temperature of 210°C, the force was 120.53 ± 13.55 N, more than 70 N greater than the removal force of a part printed with an extruder at 180°C. Varying the bed temperature, during printing and the removal process, caused an increase in the removal force from 60 to 40°C. Below 40°C, shrinkage in the printed part caused unadherence. Above this temperature, the cooling of the plastic causes an increase in the viscosity, and therefore an increase in the adhesion. These findings allow the user to balance adhesion, to prevent warping or movement of parts during the printing process, and low removal loads, to prevent excessive wear on an automated part removal mechanism.

Thesis Supervisor: Sanjay E. Sarma
Title: Professor of Mechanical Engineering

ACKNOWLEDGMENTS

The author would like to acknowledge the following people for their help and guidance through this study.

Sanjay Sarma: thesis supervisor

Emile Augustine: research assistant

TABLE OF CONTENTS

LIST OF FIGURES & TABLES

INTRODUCTION

   Invented by Charles Hull in 1983, three dimensional printing has become an important technology in the rapid prototyping and manufacturing industries (3DSystems). The 3D printing process uses a variety of technologies, among them are stereo lithography, selective laser sintering, and fused deposition modeling. This process has made it possible to produce complex geometries that would otherwise be difficult or impossible with traditional manufacturing methods. 3D printing has become the staple prototyping method due to the flexible building process and nonexistent tool-up cost.

   Fused deposition modeling (FDM), a type of 3D printing, was invented in 1989 by Scott Crump (Stratasys). After the expiration of the FDM patent about five years ago, the technology became a popular method of printing for the consumer level. This method consists of melting a thermoplastic and extruding it out of a nozzle, which moves in a horizontal plane. The extrudate is first deposited directly onto a build platform, forming the first layer. The extruder head subsequently moves up (or conversely, the build platform moves down), and plastic is extruded on top of the previous layer. This process is repeated until the extruder has reached the maximum height of the part.
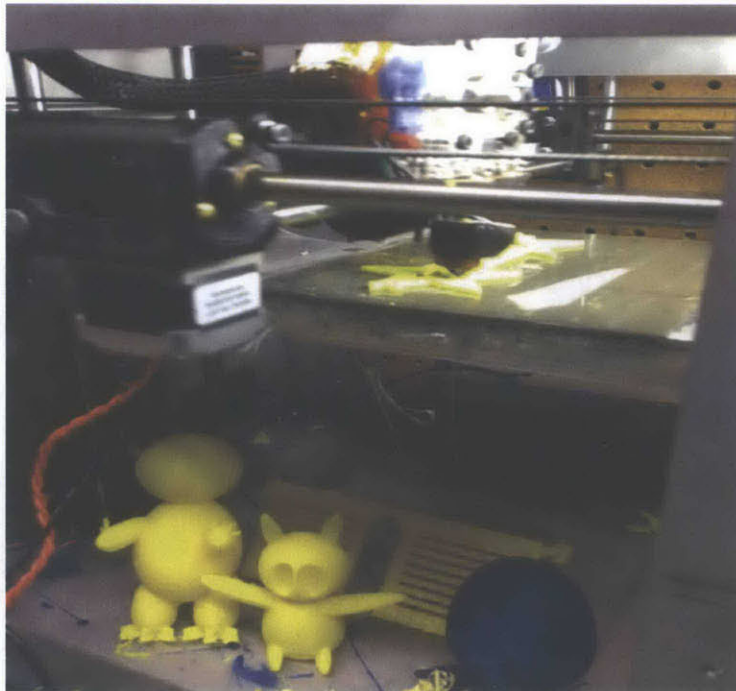
Figure 1: A *Solidoodle 2* FDM 3D printer. The printer is extruding a layer of the 3D model being created. In the foreground there are a few example parts.

BACKGROUND

FDM 3D printers are commanded using GCODE, a standard machine code for manufacturing equipment. Generating the GCODE involves converting a 3D model, usually in an STL format, using CAM (Computer Aided Manufacturing) software called a slicer. The slicer virtually slices the STL model into thin layers, which will eventually become the physical layers the 3D printer extrudes in the horizontal plane. For each layer, the slicer generates tool paths in the form of GCODE driven by a variety of parameters set by the user. Among these parameters are extruder temperature, bed temperature (build platform temperature), layer height, extrusion width, and infill density. Some of these parameters, such as layer height and infill density, control the characteristics of the printed model, while others, such as extruder temperature, are inherent to the material and printer being used. Below is a picture of a 3D model before and after slicing.

CAD Model   CAM Model
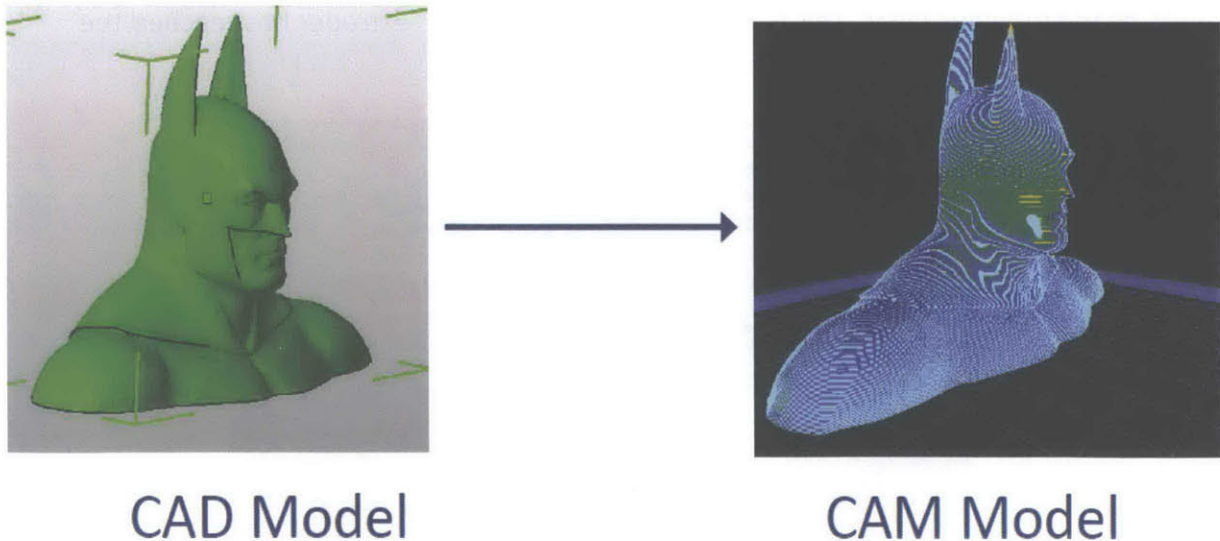
Figure 2: An STL model of batman is on the left (viewed in netfabb). A visual representation of the GCODE, generated by KISSlicer (a version of slicing software), is on the right.

Currently, most FDM printers require the user to physically remove the part from the print bed when a job is done. Most FDM printers are sold with a paint scraper, or something similar, to remove the printed model from the build platform. This inhibits 3D printers from functioning around the clock, and makes it difficult for multiple users to share them. New

Valence Robotics Corporation, a new 3D printing company, has created a patent pending removal mechanism to solve these problems. The system involves a blade, mounted to a lead screw driven robotic arm, which cuts the printed parts off of the build platform. This is similar to the manual method of using a paint scraper, the difference being that it is automated. A figure of the design is below.
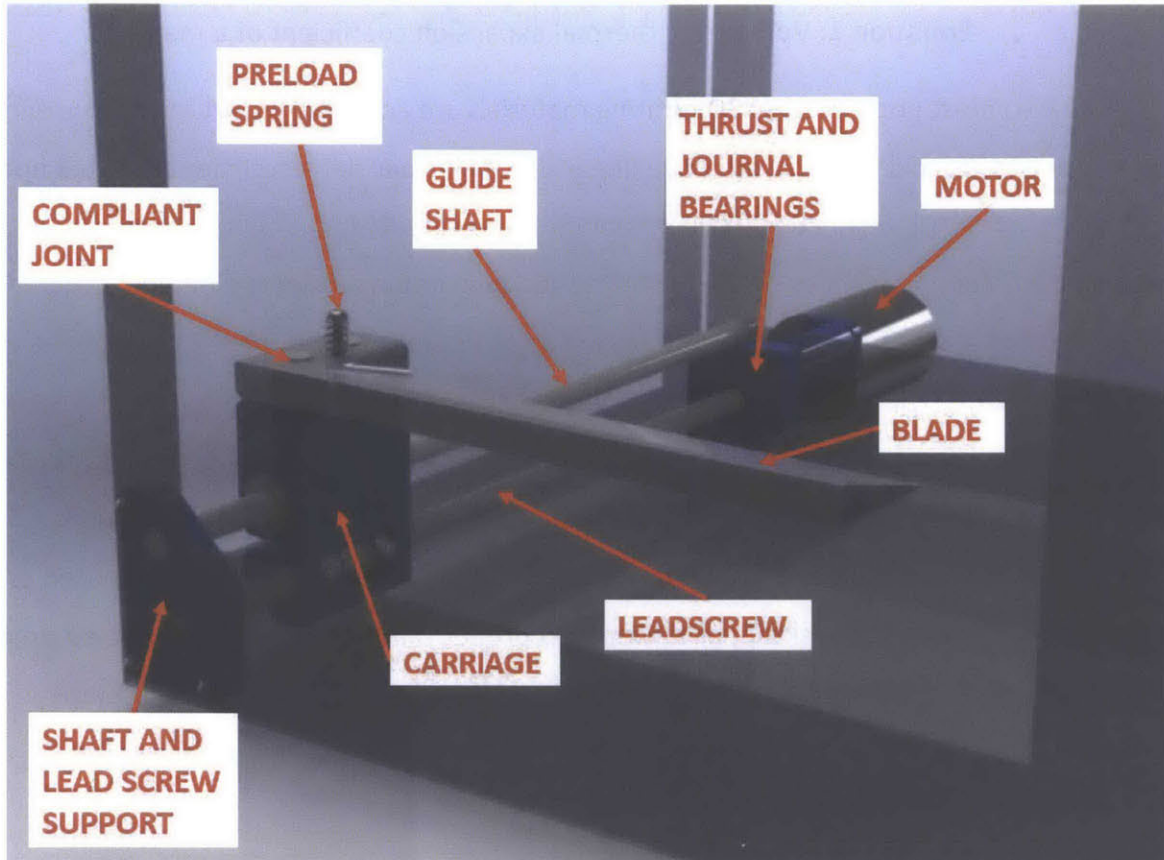
Figure 3: CAD model of the automated part removal system invented by the New Valence Robotics Corporation, consisting of a blade mounted on a lead screw driven robotic arm.

When plastic is melted in the hot end of the extruder, it expands proportionally to the thermal expansion coefficient. Conversely, when the plastic cools after being extruded on the 3D printer, it contracts or shrinks. If a part cools too much before the print is over, shrinking significantly, it may unadhere from the build platform. When this happens, a part's position can no longer be referenced to the extruder because the part is free to move, causing a failed print. There are generally two solutions to this problem. The most common solution is to use a build platform that adheres to the material being printed. Another effective solution is

using a heated build platform, which maintains a temperature close to the glass transition of the material being printed. The equation for the thermal expansion coefficient, relating the change in temperature (∂T) to the change in volume (∂V) of a material, is shown below (Eq. 1).

$$\alpha_v = \frac{1}{V} * \left(\frac{\partial V}{\partial T}\right)_p$$

Equation 1: Volumetric thermal expansion coefficient of a material.

The two most popular FDM 3D printing materials are acrylonitrile butadiene styrene (ABS) and polylactic acid (PLA), which have linear thermal expansion coefficients of 76.3 and 120. ($*10^{-6}$ K^{-1} @ 50°C), respectively (Mah, Meng). Although ABS has a higher thermal expansion coefficient, it is more prone to shrinkage when not in an actively heated environment because it has a higher glass transition temperature, and therefore solidifies at a higher temperature. The glass transition temperature of PLA is 58°C, while that of ABS is 105°C. The change in temperature from the solidification of ABS to room temperature (25°C) is a factor of 2.4 greater than that of PLA, while the coefficient of thermal expansion of PLA is only 1.6 times greater than that of ABS. It can be challenging to print ABS without a costly heated print chamber. Printing PLA on a desktop, or low end 3D printer that does not have a heated printing chamber is relatively easy. Partly for this reason, PLA is a more popular and user friendly material for most 3D printer consumers. The focus in this study is on PLA because of its consistency when printing.

There are many materials used for build platforms, including Kapton tape, ABS, masking tape, and glass. In this study, polyetherimide resin (PEI) film is used as a build platform material. It is ideal for printing because the glass transition temperature of PEI is 217°C (GE Advanced Materials), within the printing temperature range of PLA. This allows the adhesion of the printed material to the build platform material to be controlled by the printing temperature parameters. If the PLA print material is extruded close to or above the glass transition temperature of the platform material, PEI, then the platform material will significantly decrease in viscosity. Once the contacting polymers cool and harden, increasing the viscosity of both materials, a greater adherence force is generated than the case when only the extruded

material goes through a glass transition. This is the case with a build platform material of Kapton tape or glass, which both have glass transition temperatures much higher than the extrudate temperature range of PLA (DuPont).

Bed leveling and first layer height calibration are important steps to ensure that the first layer of a print is extruded evenly across the build platform, such that extrudate is slightly smeared to increase the contact area with the build platform. A larger contact area increases the adherence force. If the contact area is too small, shrinkage in the model being built will overcome the adherence force to the build platform, causing it to come loose and ruining the print. This process is usually done so that the print nozzle barely is elevated above the platform, much less than the diameter of the extrudate. In doing so, the user can be sure the adherence is maximized. This makes it more difficult for the user to remove the part, but is not an impediment. When using an automated part removal system, an excessive adherence force can be an impediment to the longevity of the system. Therefore, the adherence should be minimized to reduce the force imposed on the part removal system, but still great enough to inhibit unadherence of the part from the build platform during printing. The first layer height is usually calibrated using a set screw which makes contact with a bump sensor attached to a z-axis actuated carriage, much like the one in Figure 4 below.
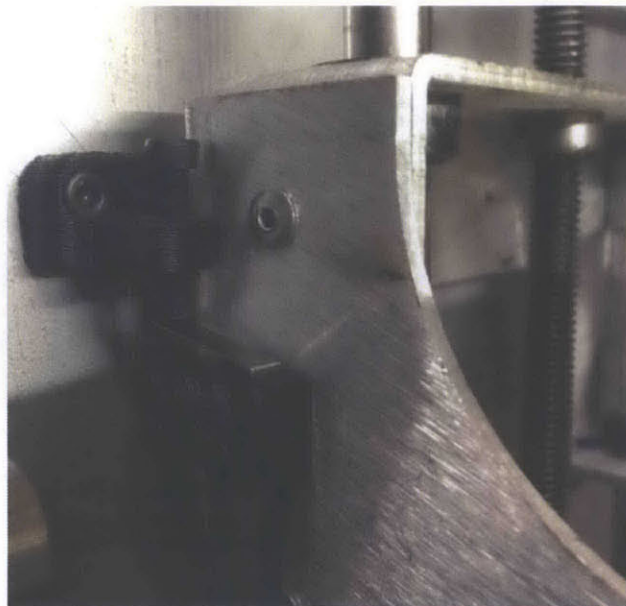
Figure 4: First layer calibration is done by moving a set screw up or down, which presses on a bump sensor attached to the z-axis actuated carriage.

PROCEDURE

In this study, the force required to remove a 3D printed part from a Solidoodle 2 3D printer was measured, varying four printing parameters and the orientation of the printed part. The removal mechanism used is similar in design to the CAD model in Figure 3, compromised of a blade, carriage, guide shaft, and lead screw. Bronze bushings, impregnated with 19% SAE 30 oil, guide the carriage along the guide shaft. A lead screw mechanism pulls the carriage, providing the force required to remove a part. The blade, which cuts the part off of the build platform, is mounted to the carriage on pegs that allow compliance for leveling. Leveling of the blade is essential to make sure the blade is relatively flush to the build platform, ensuring the blade edge cuts between the build platform and the printed part. In this study, an AWS H-110 force gauge was attached to the lead screw to measure the force during removal. Note that this is not the force experienced by the blade, but by the drivetrain, which is marginally higher because it is subject to the bushing friction. Figure 5 shows the blade before and after calibration. Figure 6 shows the force gauge pulling on the lead screw mechanism.
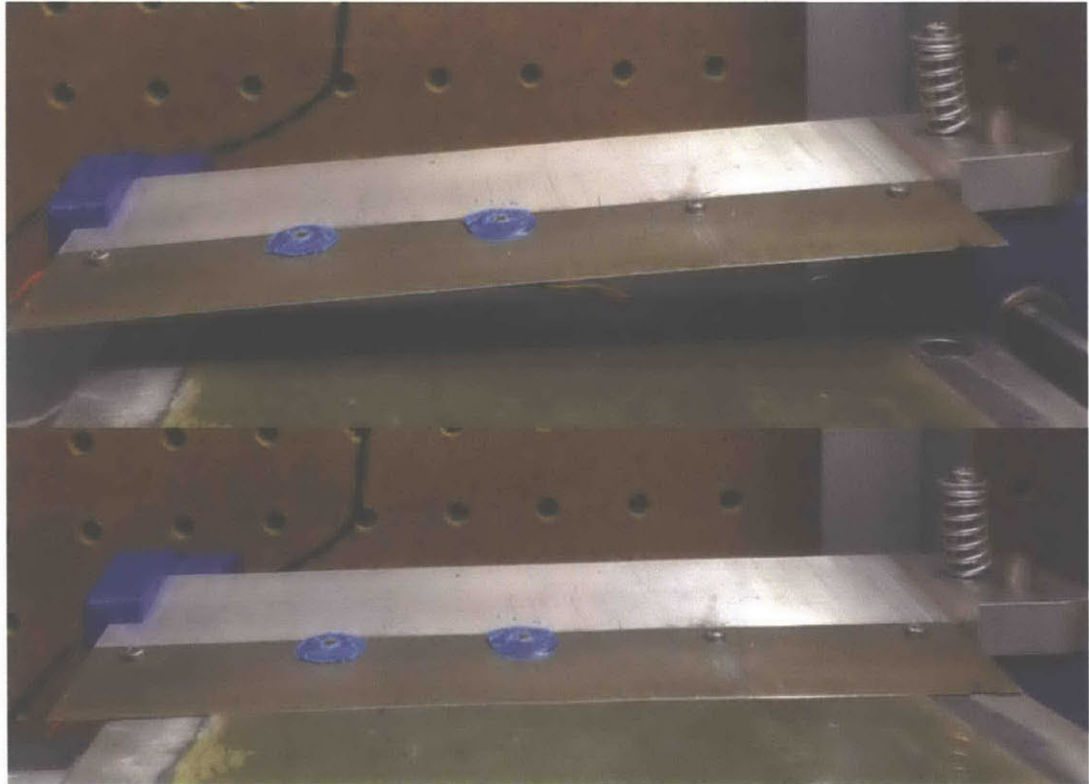
Figure 5: Compliant removal blade, before and after leveling, mounted on pegs that are inserted into the carriage.
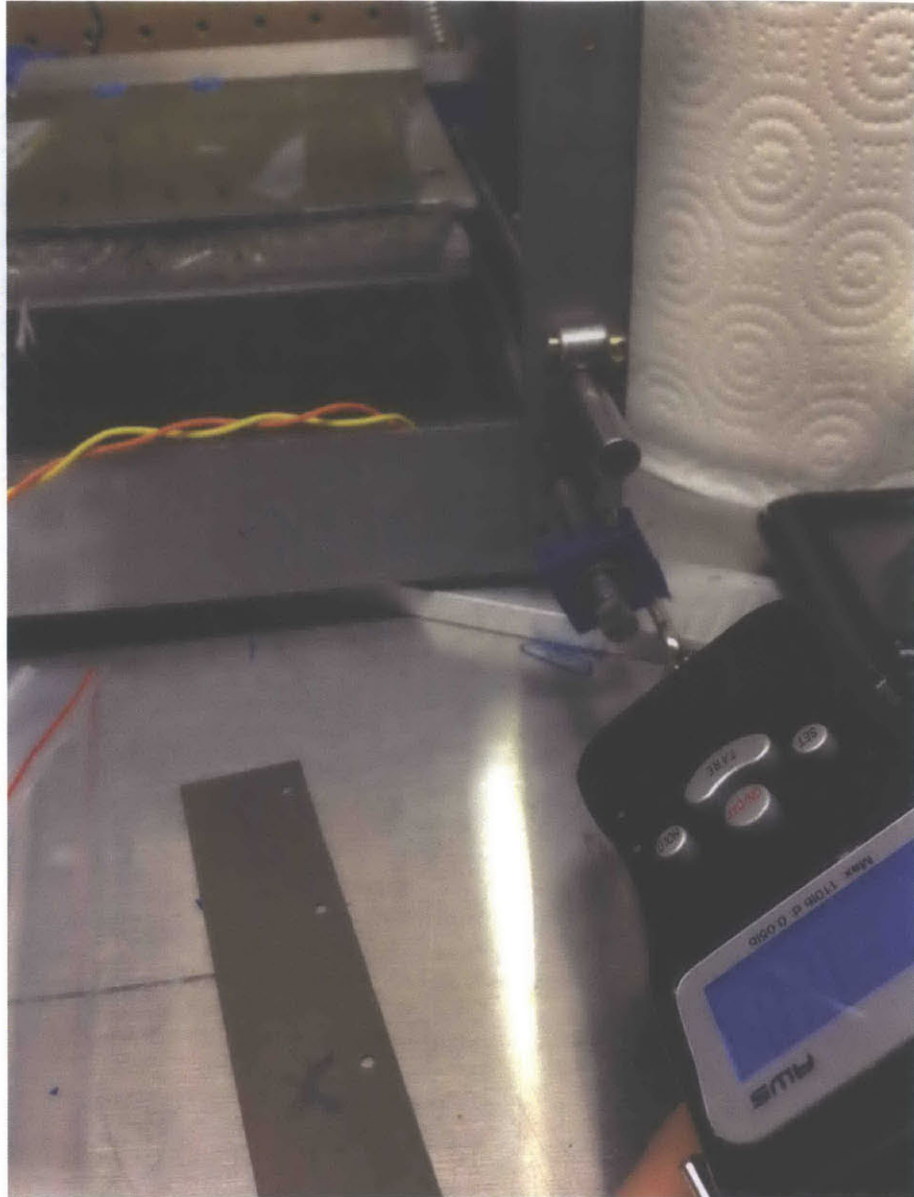
Figure 6: Force gauge attached to the lead screw mechanism that actuates the carriage-blade assembly.

The distributed preload on the blade was measured five times, with an average of 58.57 ± 2.49 N/m (confidence intervals are all to 5% significance). The friction force when dragging the leveled blade across the build platform, without an impeding part, was 6.94 ± 0.19 N. The preload ensures the blade stays flush during the removal process, but also causes the additional friction force on the blade edge and the linear bushings. The blade insert, or cutting edge, is made from 0.026" thick, HRC 56, D2 blade steel, ground at 9.5°on the bottom of the leading edge, and 29° on the top. The grinding process was done on a surface grinder (Fig. 7).
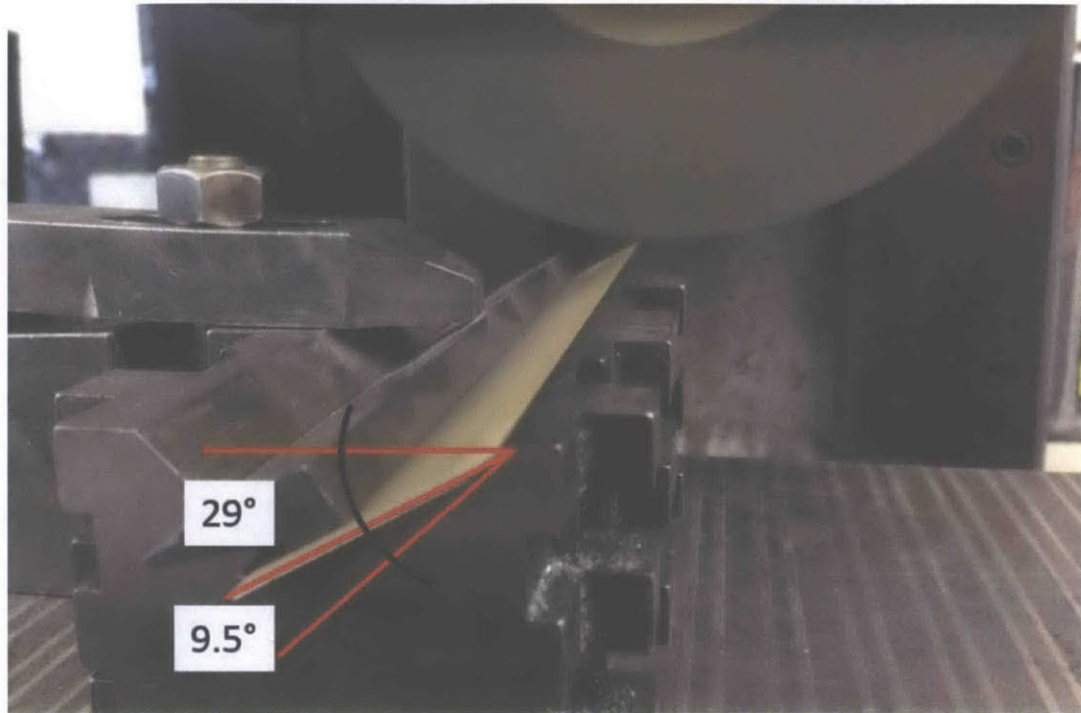
Figure 7: Surface grinding of D2 bade steel for the blade insert. The top of the leading edge is ground at 29°, the bottom at 9.5°.

The build platform is a heated aluminum plate with a PEI film glued to the surface. The General Electric made PEI film used, called ULTEM, is 0.010" thick. Sainsmart PLA was used as a printing material, which comes in one kilogram spools of 1.75mm diameter filament, designed for the extruder size on the Solidoodle 2.The extruder has a nozzle diameter of 0.35mm, from which the printing material is extruded onto the PEI build platform. Figure 8 shows a picture of the filament and build platform.
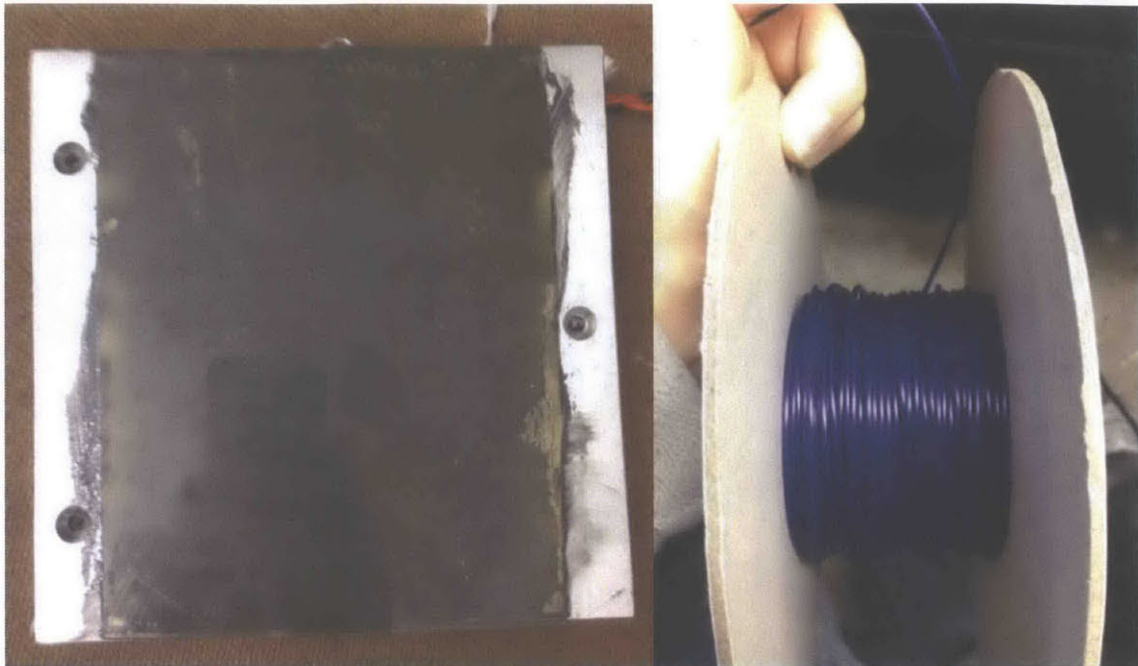
Figure 8: The aluminum build plate with PEI film glued to it is on the left. On the right is a partial spool of blue PLA filament on a spool.

The STL model used for testing was a 3mm thick ellipse shape, with major and minor axis lengths of 40mm and 20mm. For each set of printing parameter tests, the part was removed in two orientations. One with the major axis aligned with the x-axis of the printer (approximately perpendicular to the blade edge), and the other with the major axis aligned with the y-axis of the printer (approximately parallel to the blade edge). The STL model was sliced using CAM software called KISSlicer, generating the GCODE that controlled the Solidoodle 2. In this software, three of the four printing parameters were controlled. Extruder temperature was varied between 180°C and 210°C, bed temperature during printing was varied between 60°C and 30°C, and bed temperature during the removal process was varied between 60°C and 30°C. Figure 9 has a picture of the STL model as well as a visual representation of the first three layers of the GCODE (note that there are more than three layers to the entire print).
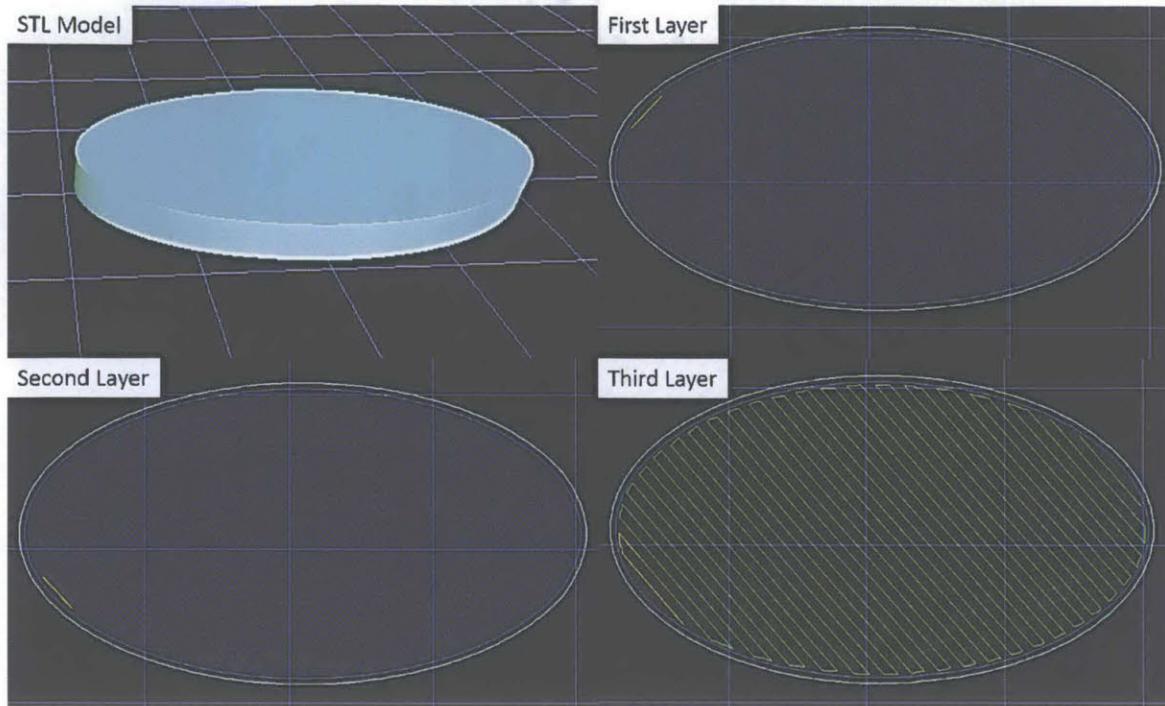
Figure 9: Visual representation of the STL model and first three layers of GCODE used for removal testing. This is a viewing window in KISSlicer.

The fourth parameter was the first layer height, controlled by the z-set screw and measured with calipers. The first layer height was varied between 0.42 ± 0.02mm and 0.18 ± 0.01mm. Printing parameters were varied independently to find correlations between the force of removal and the parameters being tested. Four increments of each parameter were tested. For each test, the two orientations of the part described above were removed from the build platform five times, measuring the maximum force each time. There were 13 printing configurations, with two part orientations each, for a total of 26 configurations. There were a total of 130 tests. Table 1 summarizes the testing configurations. The letters A through D represent each parameter's four increments. The baseline configuration, AAAA, is a set of basic printing parameters that works for most PLA parts on the Solidoodle 2. Appendix A shows the exact settings used to generate the base configuration GCODE in KISSlicer. Figure 10 shows a sample test print for each first layer height measurement.

Configuration	Bed Temperature (°C)	Extruder Temperature (°C)	First Layer Height (mm)	Removal Bed Temperature (°C)	Orientation
AAAA	60	180	0.42 ± 0.02	60	\\ & ⊦
BAAA	50	180	0.42 ± 0.02	60	\\ & ⊦
CAAA	40	180	0.42 ± 0.02	60	\\ & ⊦
DAAA	30	180	0.42 ± 0.02	60	\\ & ⊦
ABAA	60	190	0.42 ± 0.02	60	\\ & ⊦
ACAA	60	200	0.42 ± 0.02	60	\\ & ⊦
ADAA	60	210	0.42 ± 0.02	60	\\ & ⊦
AABA	60	180	0.33 ± 0.01	60	\\ & ⊦
AACA	60	180	0.27 ± 0.01	60	\\ & ⊦
AADA	60	180	0.18 ± 0.01	60	\\ & ⊦
AAAB	60	180	0.42 ± 0.02	50	\\ & ⊦
AAAC	60	180	0.42 ± 0.02	40	\\ & ⊦
AAAD	60	180	0.42 ± 0.02	30	\\ & ⊦

Table 1: Four parameters were tested independently, each with a perpendicular and parallel orientation of an ellipse to the leading edge of the removal mechanism's blade edge.

0.42 ± 0.02 mm   0.33 ± 0.01 mm

0.27 ± 0.01 mm   0.18 ± 0.01 mm
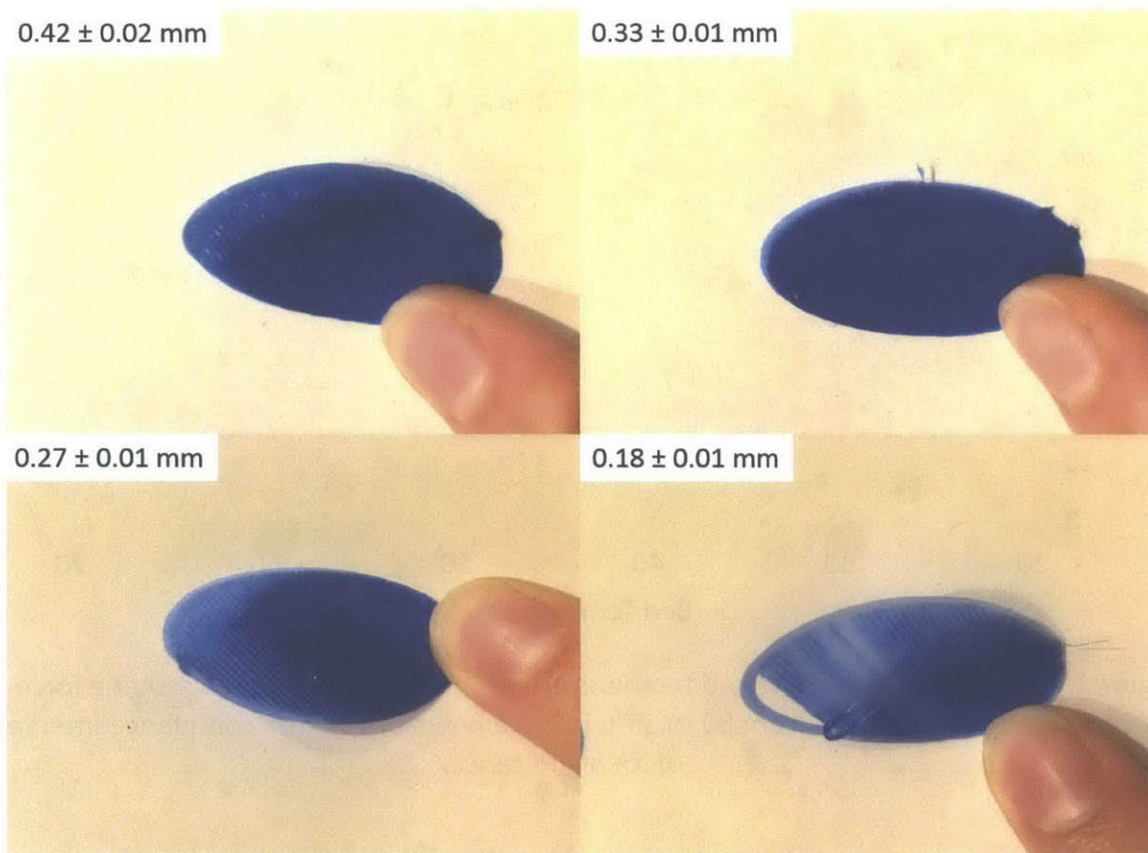
Figure 10: Sample prints from each of the layer height measurement prints. These were measured using calipers.

RESULTS

The first test was varying the bed temperature during printing. Figure 11 shows the force required to remove a part was minimized for a printing bed temperature of 60°C, and maximum with a bed temperature of 40°C. The trend lines are a quadratic fit of second order. From 30 to 40°C, removal force is increasing with bed temperature. At around 40°C, the force inflects and decreases until the final test of 60°C. Although the confidence intervals overlap, the perpendicular oriented part incurred smaller loads to the blade than the parallel orientation. The confidence intervals are greatest at the highest forces.
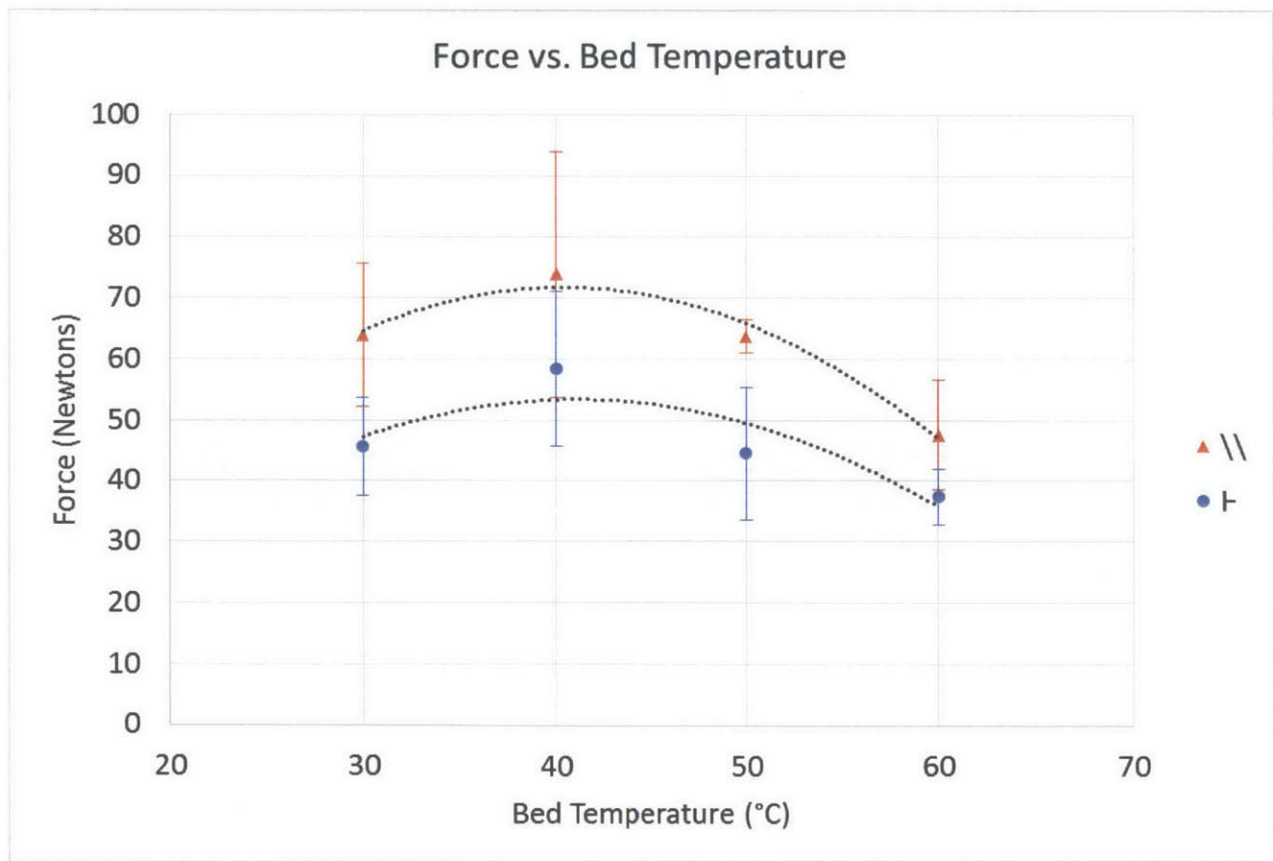
Figure 11: Data for the printing bed temperature test plotted against the resulting force. The bed temperature was varied from 60 to 30°C in increments of 10°. The confidence intervals are of 5% significance.

The extruder temperature was then varied from 180 to 210°C. From 180 to 200°C, the data rises slightly, but it is approximately linear. From 200 to 210°C, the trend of the removal force rapidly gets steeper, reaching 120.53 ± 13.55 N for the parallel orientation, and 107.42 ± 4.86 N for the perpendicular orientation. Again, the parallel orientation exhibits a larger load on the blade than the perpendicular orientation. Figure 12 shows the data for the extruder temperatures plotted against the removal force.
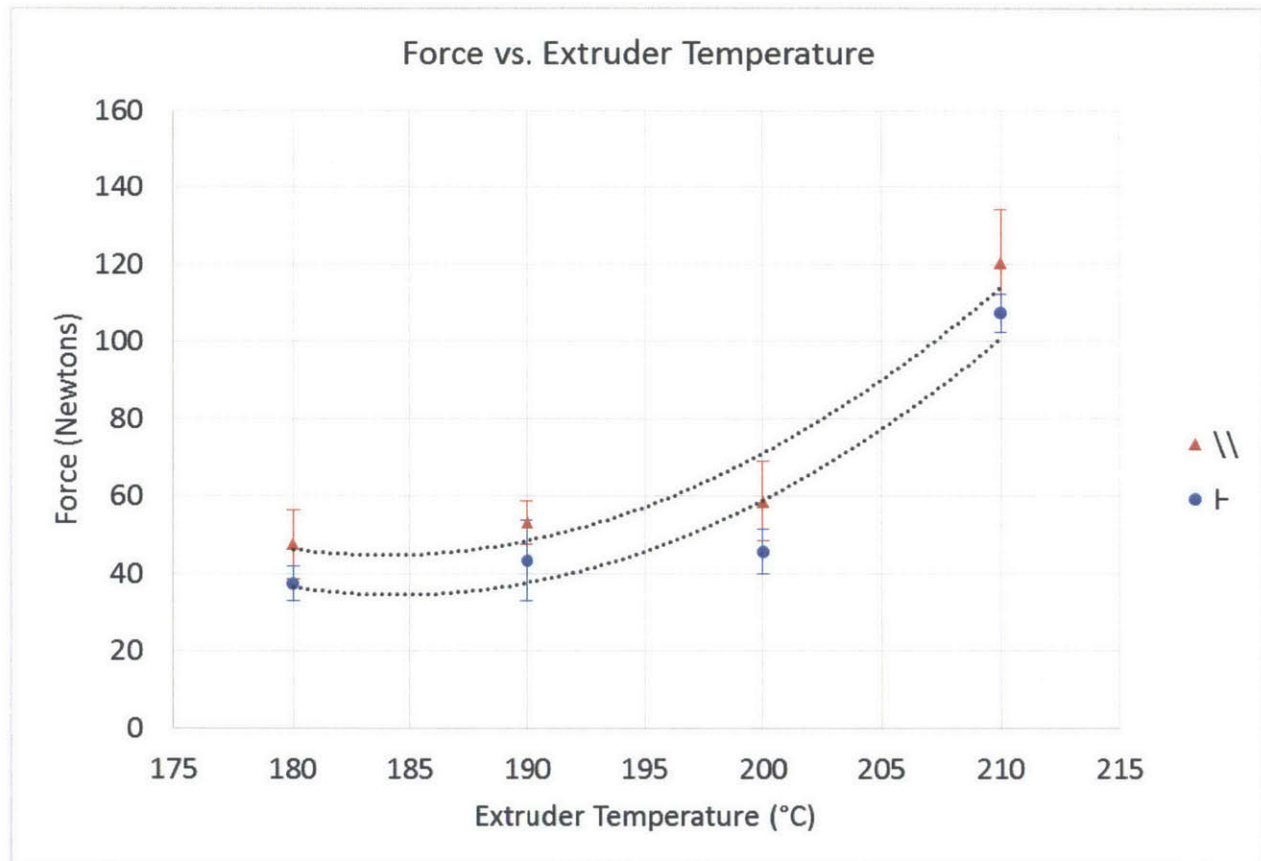
Figure 12: Data for the printing extruder temperature test plotted against the resulting force. The extruder temperature was varied from 180 to 210°C in increments of 10°.

Varying the first layer height had the greatest effect on the removal force of the four printing parameters varied. At the lowest layer height, the force reached an average of 123.92 ± 22.93 N in the parallel orientation, and 90.91 ± 24.45 N in the perpendicular orientation. In Figure 13, the trend lines suggest that the force increases approximately linearly with decreasing layer height. The data is significantly lower than the linear trend line at a layer height of 0.33 ± 0.01 mm. Again, the confidence intervals widen with increasing force.
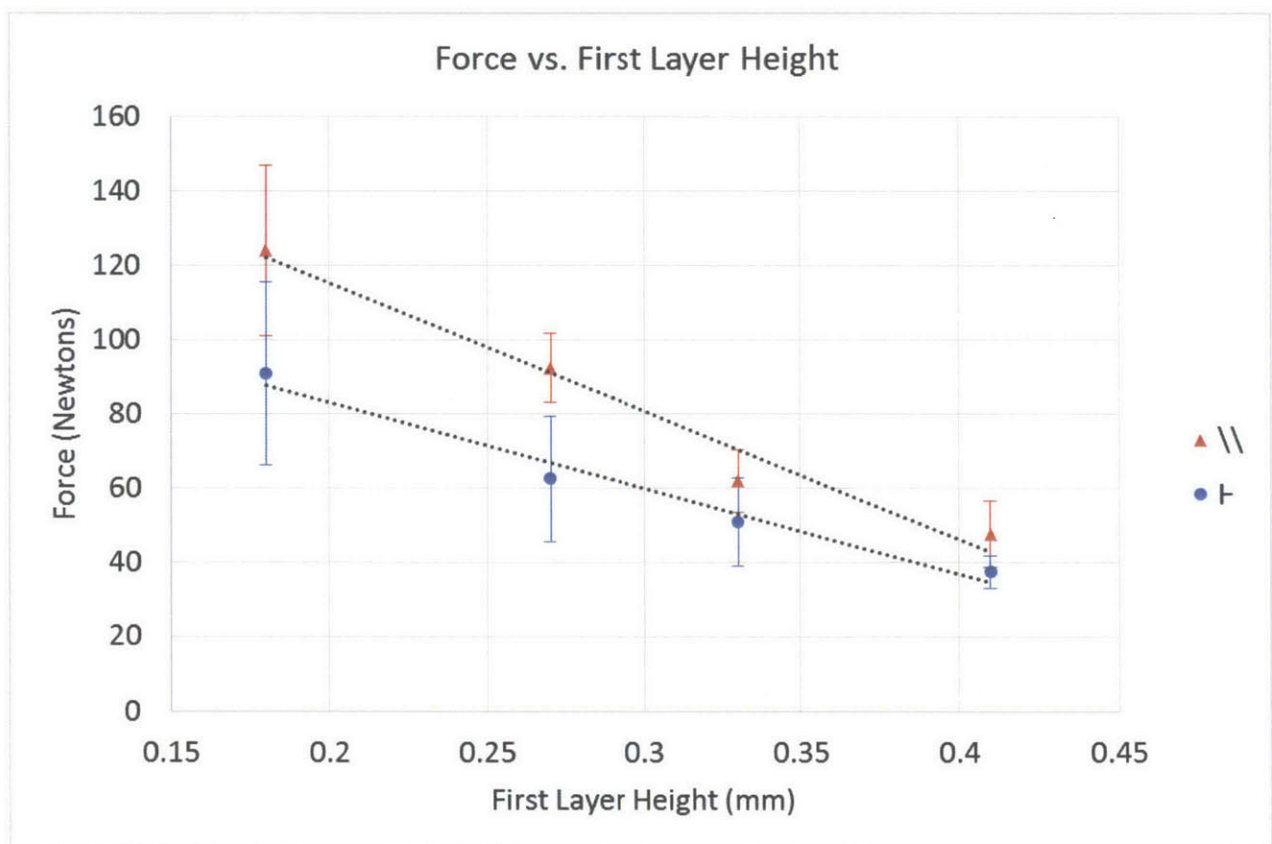
Figure 13: Data for the first layer height test plotted against the resulting removal force. The first layer height was varied from 0.18 ± 0.01 to 0.42 ± 0.02 mm.

Varying the bed temperature during the removal process had the least significant impact on the removal force compared to the other tests. In Figure 14, it can be seen that the trends have a similar shape as the printing bed temperature test, but are flatter. In this test, the maximum force for the perpendicular test was at 50°C, while it was at 40°C for the parallel case. On average, the parallel orientation caused a larger force on the blade than the perpendicular orientation.
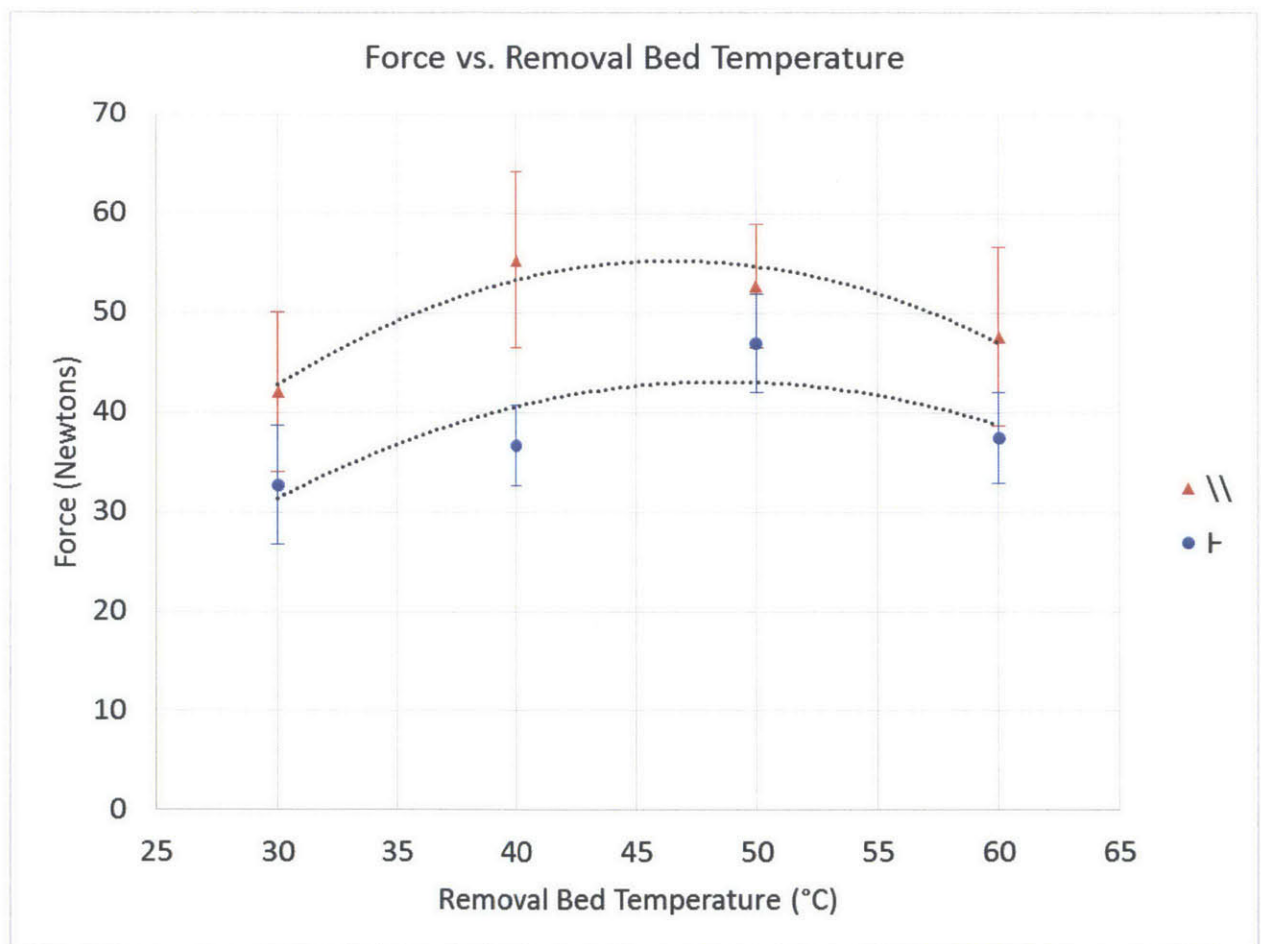
Figure 14: Data for the removal bed temperature test plotted against the resulting force. The bed temperature was varied from 30 to 60°C in increments of 10°.

The Solidoodle 2 printer is a cheap machine that is not stiff enough for repeatable printing or removal processes. During printing and removal, the build platform flexes. In addition, during the removal process, the bushings cause stick slip motion when pulling the lead screw manually, due to the bushings go back and forth between static and kinetic friction during the increase in force when the blade makes contact with the part. This leads to a step function in the force while removing the parts. Due to these factors, the printing and removal processes were not repeatable enough to make claims about the specific magnitudes of forces because the data was significantly scattered. Figure 15 shows the testing data points for the first layer height test, which had the most scatter of all the tests. At higher forces, the scatter is greater.
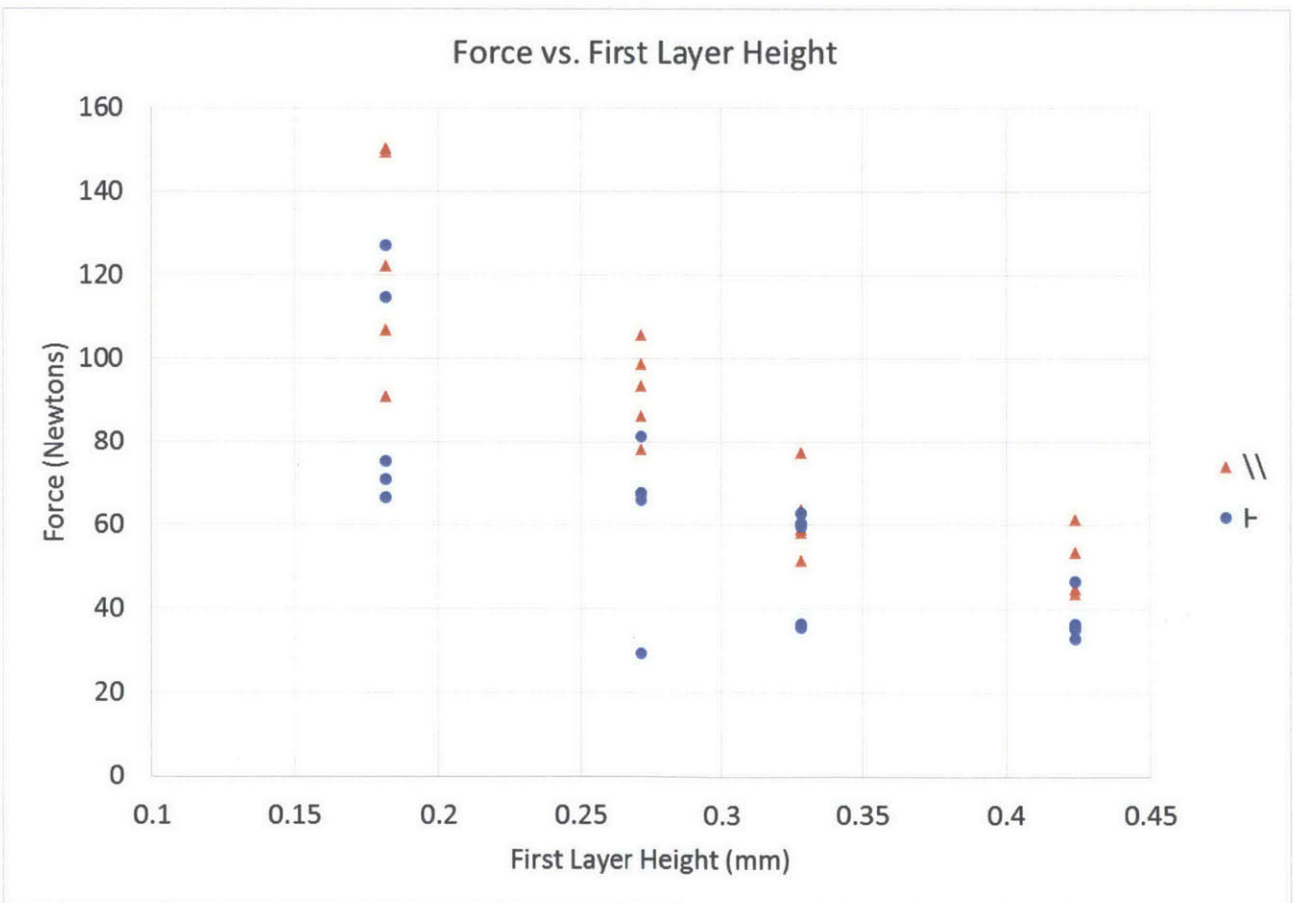
Figure 15: Raw data from the first layer height test is plotted to show the large scatter in the data. This scatter was due to the flexibility of the structure of the Solidoodle 2 3D printer, leading to a printing and removal process that were not repeatable enough to make claims on the specific magnitudes of the forces.

CONCLUSIONS

From the trends in the data presented above, inferences can be made about the driving phenomena and the optimal printing parameters when using an automated removal mechanism. Across all the tests, the force to remove a parallel oriented part was, on average, higher than a perpendicular oriented by about 10 to 20%. This is because the line of contact on the ellipse part is shorter in the perpendicular orientation than the parallel orientation. A smaller contact area leads to a more concentrated force and higher pressure. This leads to suggestion that parts should be oriented lengthwise on the build platform, with the longest axis perpendicular to the blade edge.

The printing bed temperature and removal bed temperature trends are similar, with the prior having a better fit to the quadratic trend lines. Force increased with decreasing bed temperature from 60 to 40°C. As the printed material is allowed to cool more during printing, there is a larger increase in the viscosity of the polymer. The higher the change in viscosity, the more strongly the build platform adheres to the printed part. This phenomena is overcome by shrinkage below 40°C, and is apparent in the data by a decreasing force with decreasing bed temperature below this point. When the plastic cools below 40°C, the shrinkage of the first layer reduces the adhesion between the printed part and build platform, making it easier to remove the part. This can be deduced from the thermal expansion of a material, described by Equation 1. PLA parts should be printed with a bed temperature less than about 30°C or greater than 50°C. The decision between these can be made factoring in the size of the part. If the part is large, temperature gradients can lead to warping, so the higher temperatures should be selected. If the part is small, warping is not an issue so the lower temperatures can be used to reduce power consumption.

Varying the extruder temperature around the glass transition temperature of PEI, 217°C, allows for significant control of the part adhesion to the build platform. The data in Figure 12 shows minimal change in the removal force up to about 200°C. Above this, the surface of the build platform starts to go through a glass transition, causing a significant drop in the viscosity at the surface of the PEI build platform. When the part cools and hardens, the viscosity of both the part and bed increase drastically, causing strong adhesion compared to the printing with

23

the extruder below 200°C. Selecting an extruder temperature for PLA requires considering three factors. One, if the part is large, better adhesion to the build platform can mitigate any potential warping. Two, higher adhesion forces, correlated to high extruder temperatures, puts more stress on the removal mechanism, which leads to more wear and higher chance of failure. Three, higher extruder temperatures allows each layer of the printed part to bond better, leading to stronger parts. A good extruder temperature balancing these factors is 200°C, but it can be increased or decreased to take advantage of adhesion, ease of removal, or strong parts.

The first layer height had the greatest impact on the required removal force. Reducing the first layer height does two things. Foremost, it increases the contact area of the first layer to the build platform. Area is directly proportional to the adhesion force, resulting in a linear trend. The slight deviations from the linear trend can be attributed to the proximity of the hot end of the extruder to the build platform. At lower layer heights, more heat is transferred to the build platform, slightly lowering the viscosity of the surface material. This causes more adhesion when the printed material cools and hardens. These trends lead to conclude that the first layer height should be calibrated carefully to ensure that there is enough adhesion to prevent warping, but not an excessive amount as to impede the removal process. A good value for the Solidoodle 2, which has a nozzle diameter of 0.35mm, is about 0.33mm.

The new invention of an automated part removal system has created the opportunity to optimize printing parameters for a correlation that was not significant before. Careful attention should be placed to the bed temperature, as there is a maximum. A balance of adhesion and ease of removal can be optimized for a specific model being printed by varying the extruder temperature. First layer height is a powerful variable that should be changed with precision, understanding the effect it has on the removal process. Also, since the first few layers are all that impact the removal process, a new slicing software that varies parameters for the bulk of the part and the first few layers independently would be of value. This way, any optimization in first layer height, extrusion width, or temperature for the removal process can be isolated from any optimization for the printed part.

FUTURE RECOMMENDATIIONS

Scatter is the largest concern in this study. This was due to stick slip motion of the bushings, and inconsistent printing and removing due to excessive flexing in the frame of the Solidoodle 2 printer. Using a stiffer, more consistent machine would make any study related to 3D printing more conclusive. With regards to the removal process, the most important component to the 3D printer is the z-axis guide shafts. These components are what transmit the load from the removal mechanism, through the z-carriage, to the frame of the printer. On the Solidoodle 2, there is a lot of deformation in the z-axis guide shafts when a part is being removed.

Stick slip motion lead to a step function imposed by the removal mechanism. This step function made it difficult to accurately measure the minimum required force for removal. To ensure that the force curve during a removal process is smooth, controlled motion with a constant speed is required. An experimental setup with an electrically powered drivetrain and force gauge in series would be more consistent than pulling a force gauge manually.

With more consistent data and smaller variances, commonalities and covariance could be extrapolated from cross testing multiple variables that could be confounding. The most useful test would be between extruder temperature and bed temperature because there is significant heat transfer from the nozzle to the print bed. These improvements would allow for more accurate optimization of printing parameters. Also, knowing specific magnitudes of forces under various conditions would provide constraints to design a suitable removal mechanism.

WORKS CONSULTED

3DSystems. "The Journey of a Lifetime". *3D Systems, Inc.,* 2014. Web May 2014.
< http://www.3dsystems.com/30-years-innovation>

GE Advanced Materials. "Turn up the heat, New ULTEM* film has what it takes". *General Electric Company,* 2004. Web May 2014.
< http://ultem.de/downloads/brochure_01.pdf>

DuPont. "Technical Data Sheet: Kapton HN polyimide film". *Du Pont de Nemours Company.* 2011. Web May 2014.
< http://www2.dupont.com/Kapton/en_US/assets/downloads/pdf/HN_datasheet.pdf>

Mah, Shin. "Coefficient of Thermal Expansion Test Report". *CTE Test Report,* Statasys DDM Group, 20 December, 2011. Web May 2014.
<http://www.stratasys.com/~/media/Main/Files/FDM%20Test%20Reports/Coefficient%20of%20Thermal%20Expansion%20Test%20Report.ashx>

Meng, Q.K.; Hetzer, M.; and De Kee, D. "PLA/clay/wood nanocomposites: nanoclay effects on mechanical and thermal properties". *Journal of Composite Materials,* SAGE, 22 November, 2010. Web May 2014.
< http://jcm.sagepub.com/content/early/2010/11/18/0021998310381541.full.pdf>

Stratasys. "The Invention of FDM Technology". *Stratasys Ltd,* 2014. Web May 2014.
< http://www.stratasys.com/3d-printers/technology/fdm-technology>

APPENDIX A: KISSlicer Base Configuration (AAAA) GCODE

```
; KISSlicer - FREE
; Windows
; version 1.1.0.14
; Built: May  8 2013, 11:26:16
; Running on 4 cores
;
; Saved: Sat May 03 04:34:34 2014
; 'removal_part_elipse_AAAA_parallel.gcode'
;
; *** Printer Settings ***
;
; printer_name = Solidoodle 2 Thesis
; bed_STL_filename =
; extension = gcode
; cost_per_hour = 0
; g_code_prefix = 3B205B6D6D5D206D6F64650A4732310A3B206162736F
;    6C757465206D6F64650A4739300A
; g_code_warm = 3B2053656C6563742065787472756465722C207761726D
;    2C2070757267650A0A3B2035442D7374796C650A543C4558542B303E
;    0A4D31393020533C4245443E0A4D31303920533C54454D503E0A4732
;    380A4739310A473120453830204633300A4739300A4D3832
; g_code_cool = 3B2047756172616E746565642073616D65206578747275
;    6465722C20636F6F6C696E6720646F776E0A0A3B2035442D7374796C
;    650A4D31303420533C54454D503E0A
; g_code_N_layers = 3B204D6179962652072652D686F6D65205820262059
;    3F
; g_code_postfix = 3B20416C6C20757365564206578747472756465273206
;    1726520616C72656164792027436F6F6C6564720746F20300A4D313
;    03420533138300A4D313930205336300A4732380A4730205A3133300
;    A4730205A3131302E32
; post_process = NULL
; every_N_layers = 0
; num_extruders = 1
; firmware_type = 2
; add_comments = 1
; fan_on = M106
; fan_off = M107
; fan_pwm = 0
; add_m101_g10 = 0
; z_speed_mm_per_s = 3.5
; z_settle_mm = 0.25
; bed_size_x_mm = 150
; bed_size_y_mm = 150
; bed_size_z_mm = 150
; bed_offset_x_mm = 95
; bed_offset_y_mm = 45
```

```
; bed_offset_z_mm = 0
; bed_roughness_mm = 0
; travel_speed_mm_per_s = 120
; first_layer_speed_mm_per_s = 50
; dmax_per_layer_mm_per_s = 30
; xy_accel_mm_per_s_per_s = 1500
; lo_speed_perim_mm_per_s = 20
; lo_speed_solid_mm_per_s = 40
; lo_speed_sparse_mm_per_s = 35
; hi_speed_perim_mm_per_s = 70
; hi_speed_solid_mm_per_s = 80
; hi_speed_sparse_mm_per_s = 75
; ext_gain_1 = 1
; ext_material_1 = 2
; ext_axis_1 = 0
; ext_gain_2 = 1
; ext_material_2 = 0
; ext_axis_2 = 0
; ext_gain_3 = 1
; ext_material_3 = 0
; ext_axis_3 = 0
; model_ext = 0
; support_ext = 0
; support_body_ext = 0
; raft_ext = 0
; solid_loop_overlap_fraction = 0.5
;
; *** Material Settings for Extruder 1 ***
;
; material_name = PLA
; g_code_matl = 3B204D617962652073657420736F6D65206D6174657269
;    616C2D737065636369666669320472D636F64653F
; fan_Z_mm = 0
; fan_loops_percent = 100
; fan_inside_percent = 0
; fan_cool_percent = 100
; temperature_C = 180
; keep_warm_C = 150
; first_layer_C = 180
; bed_C = 60
; sec_per_C_per_C = 0
; flow_min_mm3_per_s = 0.01
; flow_max_mm3_per_s = 10
; destring_suck = 1.25
; destring_prime = 1.25
; destring_min_mm = 1
; destring_trigger_mm = 100
; destring_speed_mm_per_s = 15
```

```
; Z_lift_mm = 0
; min_layer_time_s = 10
; wipe_mm = 10
; cost_per_cm3 = 0
; flowrate_tweak = 0.75
; fiber_dia_mm = 1.76
; color = 0
;
; *** Style Settings ***
;
; style_name = Thesis A
; layer_thickness_mm = 0.35
; extrusion_width_mm = 0.37
; num_loops = 2
; skin_thickness_mm = 0.74
; infill_extrusion_width = 0.39
; infill_density_denominator = 8
; stacked_layers = 1
; use_destring = 1
; use_wipe = 1
; loops_insideout = 0
; infill_st_oct_rnd = 1
; inset_surface_xy_mm = 0
; seam_jitter_degrees = 0
; seam_depth_scaler = 0.5
;
; *** Support Settings ***
;
; support_name = None
; support_sheathe = 0
; support_density = 0
; support_inflate_mm = 0
; support_gap_mm = 0.5
; support_angle_deg = 70
; support_z_max_mm = -1
; sheathe_z_max_mm = -1
; raft_mode = 0
; prime_pillar_mode = 0
; raft_inflate_mm = 0
;
; *** Actual Slicing Settings As Used ***
;
; layer_thickness_mm = 0.35
; extrusion_width = 0.37
; num_ISOs = 2
; wall_thickness = 0.74
; infill_style = 20
; support_style = 0
```

```
; support_angle = 69.9
; destring_min_mm = 1
; stacked_infill_layers = 1
; raft_style = 0
; extra_raft_depth = 0
; oversample_res_mm = 0.125
; crowning_threshold_mm = 1
; loops_insideout = 0
; solid_loop_overlap_fraction = 0.5
; inflate_raft_mm = 0
; inflate_support_mm = 0
; model_support_gap_mm = 0.5
; infill_st_oct_rnd = 1
; support_Z_max_mm = 1e+020
; sheathe_Z_max_mm = 0
; inset_surface_xy_mm = 0
; seam_jitter_degrees = 0
; seam_depth_scaler = 0.5
; Speed vs Quality = 0.14
; Perimeter Speed = 63.00
; Solid Speed = 74.40
; Sparse Speed = 69.40
;
; Estimated Build Time:   3.89 minutes
; Estimated Build Volume: 1.620 cm^3
; Estimated Build Cost:   $0.00
```